Observations of Radio Magnetars with the Deep Space Network

Aaron B. Pearlman,[1,*] Walid A. Majid,[2,1] and Thomas A. Prince[1,2]

[1]*Division of Physics, Mathematics, and Astronomy, California Institute of Technology, Pasadena, CA 91125, USA*
[2]*Jet Propulsion Laboratory, California Institute of Technology, Pasadena, CA 91109, USA*

The Deep Space Network (DSN) is a worldwide array of radio telescopes that supports NASA's interplanetary spacecraft missions. When the DSN antennas are not communicating with spacecraft, they provide a valuable resource for performing observations of radio magnetars, searches for new pulsars at the Galactic Center, and additional pulsar-related studies. We describe the DSN's capabilities for carrying out these types of observations. We also present results from observations of three radio magnetars, PSR J1745–2900, PSR J1622–4950, and XTE J1810–197, and the transitional magnetar candidate, PSR J1119–6127, using the DSN radio telescopes near Canberra, Australia.

I. INTRODUCTION

Magnetars are young neutron stars with very strong magnetic fields ($B \approx 10^{13}$–10^{15} G). They have rotational periods between $\sim$2–12 s and larger than average spin-down rates compared to other pulsars, placing them in the top right region of the P–$\dot{P}$ diagram (see Figure 1). Magnetars are primarily powered by the decay of their enormous magnetic fields, which serves as an energy source for their transient emission behavior [1–3]. It is thought that magnetars comprise at least 10% of the young neutron star population [4], and they tend to be more concentrated toward the inner part of the Galaxy [5].

There are currently 29 known magnetars and 2 additional magnetar candidates (normally rotation-powered pulsars), the latter exhibiting episodes of magnetar-like behavior. More than $\sim$2600 pulsars have been discovered, but only four of these are radio magnetars: PSR J1745–2900, PSR J1622–4950, XTE J1810–197, and 1E 1547.0–5408. Thus, radio magnetars are exceptionally rare and constitute $\lesssim$ 0.2% of the pulsar population. They also have large dispersion measure (DM) and Faraday rotation measure (RM) values compared to ordinary radio pulsars, which suggest that they inhabit extreme magneto-ionic environments (see Figure 2). A detailed list of properties associated with known magnetars can be found in the McGill Magnetar Catalog[3] [5].

Radio magnetars often have flat or inverted radio spectra, and their radio emission is highly linearly polarized (e.g., [6–10]). As a result, they are capable of being detected at very high radio frequencies (e.g., [7, 11, 12]). The flux densities, spectral indices, and pulse shapes of radio magnetars can also change on short timescales (e.g., [8, 10, 13–18]), and their radio pulse profiles often display multiple emission components, which can vary significantly across multiple radio frequencies (e.g., [6, 13, 18–21]). Individual pulses from radio magnetars are typically comprised of narrow sub-pulses, which can be exceptionally bright. However, they are unlike the giant pulses emitted by the Crab pulsar [6, 18, 22]. The morphology of these pulses can also change substantially between rotations (e.g., [6, 18]). Irregular timing behavior, including glitches (sudden increases in the pulsar's rotation frequency), is also commonly observed from radio magnetars (e.g., [13, 20, 21, 23–26]), and their radio emission has been reported to episodically disappear and suddenly reactivate [21, 27–32]. Radio active and quiescent magnetars can also emit short X-ray bursts [25, 33–35]. The assortment of behavior listed here points to an underlying connection between high magnetic field radio pulsars and magnetars [6, 18, 25, 31].

In this paper, we discuss recent observations of three radio magnetars, PSR J1745–2900, PSR J1622–4950, XTE J1810–197, and the transitional magnetar candidate, PSR J1119–6127, using the Deep Space Network (DSN) radio telescopes. This paper is not intended to be a comprehensive review of the vast literature on radio magnetars. Instead, we focus on recent observational results on these particular radio magnetars using the DSN antennas. For a more complete review of magnetars, we refer the interested reader to some of the available review articles on the subject (e.g., [4, 36–41]). In Section II, we describe the DSN radio dishes and the system's observing capabilities. We discuss our observational results on each of the four magnetars listed above in Sections III–VI. A summary is provided in Section VII. This paper was prepared in response to an invited solicitation for a dedicated special issue on magnetars.

II. THE DEEP SPACE NETWORK

The DSN consists of an array of radio telescopes at three locations (Goldstone, California; Madrid, Spain; and Canberra, Australia). Each of these sites is approximately equally separated in terrestrial longitude and situated in a relatively remote location to shield against radio-frequency interference (RFI). With multiple radio antennas at each site, the DSN covers both celestial hemispheres and serves as the spacecraft tracking and communication infrastructure for NASA's deep space missions. The three DSN complexes each include a 70 m diameter antenna, with a surface suitable for radio observations at frequencies up to 27 GHz. In addition, each site hosts a number of smaller 34 m diameter radio telescopes, which are capable of observations as high as 32 GHz. Each antenna is equipped with multiple high efficiency feeds, highly sensitive cryogenically cooled receivers, and dual (circular) polariza-

---

* aaron.b.pearlman@caltech.edu; NDSEG Research Fellow; NSF Graduate Research Fellow.
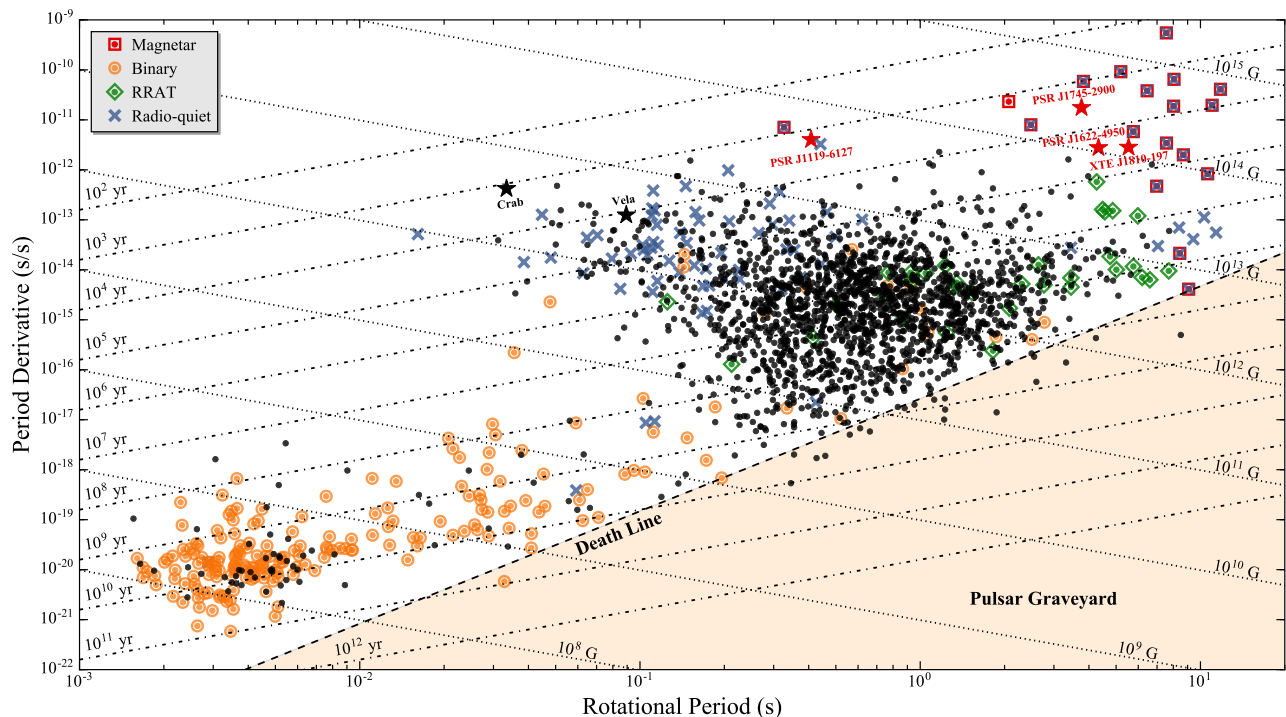[3] See http://www.physics.mcgill.ca/~pulsar/magnetar/main.html.

FIG. 1. P–$\dot{P}$ diagram of pulsars in the Australia Telescope National Facility (ATNF) pulsar catalog[a] [42]. The four radio magnetars, PSR J1745–2900, PSR J1119–6127, PSR J1622–4950, and XTE J1810–197, discussed in this paper are labeled using red stars. Magnetars (red squares), rotating radio transients (RRATs; green diamonds), and millisecond pulsars (MSPs; orange circles) are also shown, along with the population of rotation-powered radio pulsars (black circles). Radio-quiet pulsars are indicated with blue crosses and include many of the magnetars shown in red. Lines of constant magnetic field and characteristic age are derived assuming a constant braking index of $n = 3$. The radio pulsar death line is given by the model in Equation (4) of Zhang *et al.* [43].

[a] See https://www.atnf.csiro.au/people/pulsar/psrcat.

tion capabilities. When the DSN antennas are not communicating with spacecraft, they may be used for radio astronomy and other radio science applications.

Recently, all three sites have been upgraded with state-of-the-art pulsar processing backends that enable data recording with high time and frequency resolution. The DSN telescopes are able to perform radio observations at the following standard frequency bands: L-band (centered at 1.5 GHz), S-band (centered at 2.3 GHz), X-band (centered at 8.4 GHz), and Ka-band (centered at 32 GHz). In addition, the 70 m radio dish in Canberra (see Figure 4) is outfitted with a dual beam K-band feed covering 17–27 GHz. These capabilities are currently being used in various pulsar-related programs, which include high frequency, ultra-wide bandwidth searches for pulsars in the Galactic Center (GC), high frequency monitoring of radio magnetars [16–18, 31, 32, 45–47], multifrequency studies of giant pulses from the Crab pulsar [48, 49], and high frequency searches for fast radio bursts (FRBs).

The DSN radio telescopes are particularly well-suited for monitoring radio magnetars. These instruments allow for high cadence observations, which are important for tracking changes in the flux densities, pulse profile shapes, spectral indices, and single pulse behavior of radio magnetars, all of which can vary on daily timescales. High frequency observa-

tions are also essential because the spectral indices of radio magnetars are quite flat or inverted on average. In fact, the GC magnetar, PSR J1745–2900 (see Section III), has been detected at record high radio frequencies [11, 12]. The DSN antennas are also capable of providing simultaneous, dual band observations with both circular polarizations, which is essential for accurate spectral index measurements and polarimetric studies. Additionally, since the large 70 m dishes have very low system temperatures, they are ideal for studying the morphology of single pulses from radio magnetars. We refer the reader to several of our recent papers (see [16–18, 31, 32, 45–49]), which are summarized in Sections III–VI.

III. PSR J1745–2900: THE GALACTIC CENTER MAGNETAR

The GC magnetar, PSR J1745–2900, was serendiptiously discovered by the Neil Gehrels *Swift* Observatory after a hard X-ray burst was detected on 2013 April 24 [33, 34]. The magnetar has DM (1778 ± 3 pc cm^{-3}) and RM (-66960 ± 50 rad m^{-3}) values that are larger in magnitude than any known pulsar [50] (see Figure 3). It is located ~ 0.1 pc from the Galaxy's central $4 \times 10^6 \, M_\odot$ black hole, Sagittarius A* (Sgr A*) [51], making it an excellent probe of
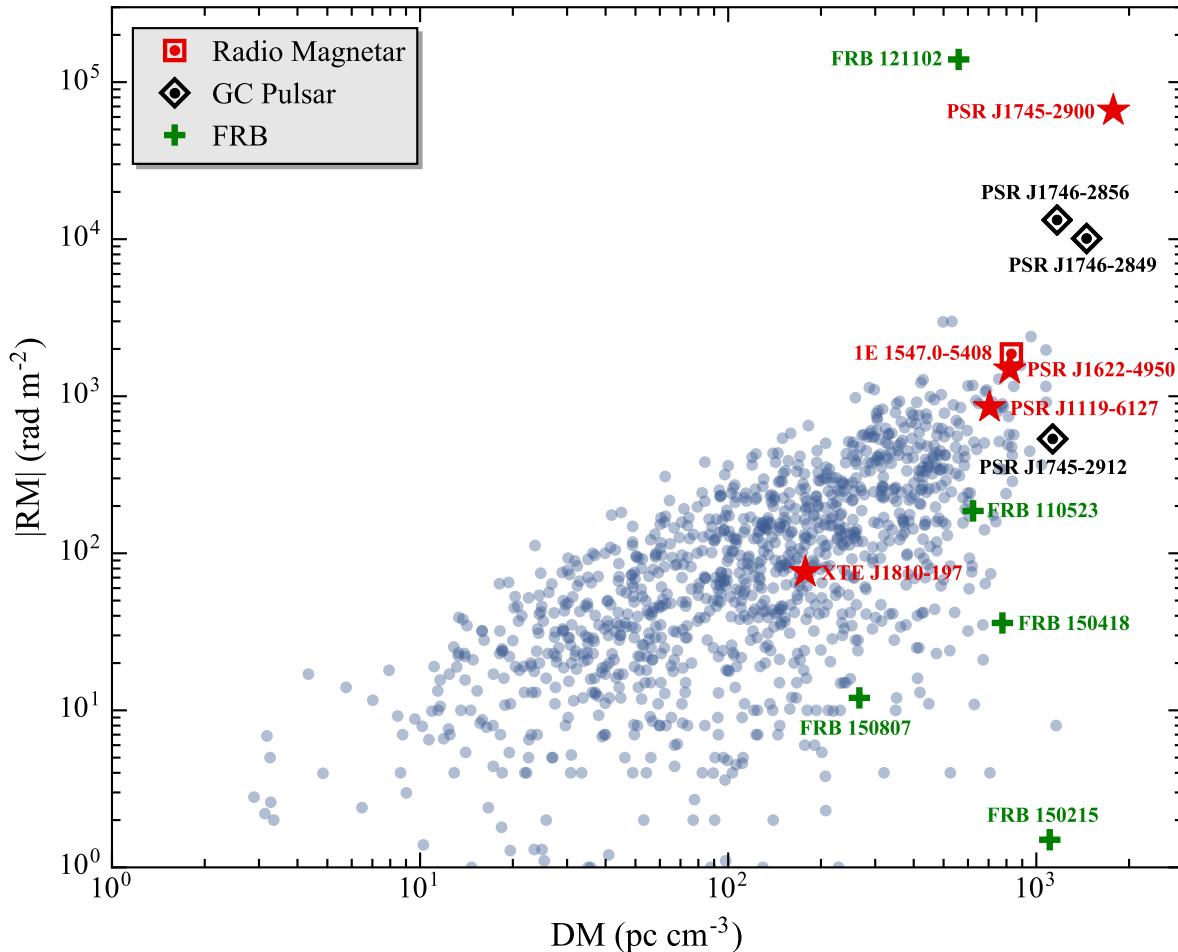
FIG. 2. Magnitude of the Faraday rotation measure (RM) versus dispersion measure (DM) for all known pulsars (blue circles) in the Australia Telescope National Facility (ATNF) pulsar catalog[a] [42]. We label the four radio magnetars considered in this paper, PSR J1745–2900, PSR J1119–6127, PSR J1622–4950, and XTE J1810–197, using red stars. The one other radio magnetar, 1E 1547.0–5408, is indicated by a red square. We also show the Galactic Center (GC) pulsars using black diamonds and the four fast radio bursts (FRBs) with RM measurements in the FRB catalog[b] [44] using green crosses.

[a] See https://www.atnf.csiro.au/people/pulsar/psrcat.
[b] See http://frbcat.org.

the magneto-ionic environment near the inner region of the Galaxy. We recently carried out simultaneous radio observations of PSR J1745–2900 at 2.3 and 8.4 GHz during four separate epochs between 2015 July 30 and 2016 August 20 using the 70 m DSN radio telescope, DSS-43 (see Section II) [18]. The observational parameters used for this study are provided in Pearlman et al. [18]. Here, we discuss our measurements of the magnetar's radio profile shape, flux density, radio spectrum, and single pulse behavior, which are also described in detail in Pearlman et al. [18].

Radio pulsations were detected at a period of $P \approx 3.77$ s in all of our observations [18]. The average X-band pulse profiles, shown in Figure 4, are single-peaked during epochs 1–3 and double-peaked during epoch 4. The S-band pulse profiles are not shown here since the pulsed emission was significantly weaker at this frequency. The mean flux density at S-band was noticeably variable [18], and the X-band

flux densities on 2015 July 30 and August 15 were smaller by a factor of $\sim$7.5 compared to measurements performed $\sim$5 months earlier by Torne et al. [12]. Our measurements on 2016 April 1 and August 20 indicated that the X-band flux density more than doubled since 2015 August 15 [18].

Multifrequency radio observations of PSR J1745–2900 revealed that its radio spectrum is often relatively flat or inverted [11, 12, 50], which is typical of most radio magnetars. However, its radio spectrum can also significantly steepen to levels comparable to ordinary radio pulsars [18, 52], which have an average spectral index of $\langle \alpha \rangle = -1.8 \pm 0.2$ [53]. During epochs 1–3, Pearlman et al. [18] found that the magnetar exhibited a significantly negative average spectral index of $\langle \alpha \rangle = -1.86 \pm 0.02$ when the average pulse profile was single-peaked, which is comparable to the steep spectrum derived by Pennucci et al. [52] between 2 and 9 GHz. The spectral index then significantly flattened to $\alpha > -1.12$ during epoch 4

FIG. 3. Image of the Canberra Deep Space Communication Complex (CDSCC). The 70 m telescope (DSS-43) is shown in the foreground and the three 34 m beam waveguide antennas (DSS-34, DSS-35, and DSS-36) are shown in the background. Image credit: CDSCC[a].

[a] See https://www.cdscc.nasa.gov/Pages/antennas.html.

when the profile displayed an additional component [18].

Pearlman *et al.* [18] also performed an analysis of single pulses detected at 8.4 GHz during epoch 3, which displayed the brightest pulses. They found that the single pulse structure observed from the GC magnetar was extremely variable in time, and the pulse morphology can be entirely different between successive rotations [18] (e.g., see Figure 5). Giant pulses, with flux densities more than ten times the mean flux level, and pulses with multiple emission components were detected during many of the magnetar's rotations [18]. These giant pulses are different in nature from those emitted by the Crab pulsar [22]. There is also some evidence that the brightest emission component appears first during a given rotation and may trigger additional weaker outbursts [18].

The observed flux density distribution of the single pulses could not be described by a log-normal distribution due to these giant pulses, and bright single pulses can sometimes form a high flux tail [18, 54]. This is similar to the single pulse behavior reported from the transient radio magnetar, XTE J1810–197, whose pulse-energy distribution is well described by a log-normal distribution at lower energies and a power-law at higher energies [55]. In particular, Pearlman *et al.* [18] measured a scaling exponent of $\Gamma = -7 \pm 1$ from a power-law fit to the distribution of single pulse flux den-

sities with peak fluxes greater than 15 times the mean level. The pulse intensity distribution is likely variable in time since a high flux tail has not persistently been observed from the GC magnetar [18, 54, 56, 57]. No correlation has been found between the peak flux density and the number of emission components in the single pulses [18]. In addition, an earlier single pulse analysis by Yan *et al.* [56] at 8.6 GHz revealed no obvious correlation between the width and the peak flux density of the GC magnetar's strongest pulses, and there was no evidence indicating sub-pulse drifting in their observations.

Pearlman *et al.* [18] found that the typical intrinsic pulse width of the emission components was $\sim$1.8 ms, and they reported a prevailing delay time of $\sim$7.7 ms between successive components. Additionally, their analysis showed that some of the emission components at later pulse phases were detected more strongly in one of the circular polarization channels, which suggests that some of the magnetar's emission components may be more polarized than others (e.g., see Figure 5(b)) [18]. The overall single pulse behavior during epoch 3 can be explained by fan beam emission with a width of $\pm 7°$, and tapering of the fan beam may give rise to fainter emission components at later pulse phases [18].

The GC magnetar's emission region is thought to emit pulses fairly regularly since bright single pulses were detected

during almost all rotations. During epoch 3, bright pulses were detected during $\sim$70% of the GC magnetar's rotations, but often not at precisely the same phase [18]. At higher radio frequencies ($\sim$45 GHz), Gelfand *et al.* [57] found that bright pulses, with an average width of $\sim$4.6 ms, were produced during a similar fraction of the magnetar's rotations. However, radio observations at 3.1 GHz have shown that the GC magnetar can exhibit brief periods of pulsar nulling [58]. Strong single pulses have also been detected at radio frequencies up to 154 GHz [11], which suggests a broadband underlying emission mechanism.

Pearlman *et al.* [18] discovered significant frequency structure over bandwidths of $\sim$100 MHz in many of the single pulse emission components, which is the first time such behavior has been observed from a radio magnetar. They argued that these features could be produced by strong lensing from refractive plasma structures located near the inner part of the Galaxy, but may also be intrinsic to the magnetar and possibly similar to the banded structures observed in the Crab pulsar's High-Frequency Interpulse [59]. Diffractive interstellar scintillation and instrumental effects were both ruled out as possible origins of this behavior [18]. If these features are indeed due to interstellar plasma lensing, then this suggests that a magneto-ionic medium close to the GC can boost the observed flux densities of pulses by more than an order of magnitude [18]. This behavior is reminiscent of the structure observed in pulses from the repeating FRB 121102 [60–62] and may indicate a connection with the larger population of FRBs. Furthermore, the GC magnetar and the repeating FRB 121102 have similar DM and RM values (see Figure 2) and emit pulses with similar morphology. An extragalactic magnetar near a massive black hole, perhaps not unlike PSR J1745–2900, is one of the currently favored progenitor theories for FRBs (e.g., [62–64]).

Recently, Pearlman *et al.* [18] showed that the emission components comprising the GC magnetar's single pulses can be substantially broadened (e.g., see Figure 5(a)). A characteristic single pulse broadening timescale of $\langle \tau_d \rangle = 6.9 \pm 0.2$ ms was reported at 8.4 GHz [18]. The pulse broadening magnitude was also found to be variable between pulses detected during consecutive pulse cycles and between pulse components in the same pulsar rotation [18]. Pearlman *et al.* [18] argued that this behavior could be intrinsic, a result of multiple successive unresolved low amplitude emission components, or extrinsic to the magnetar, possibly produced by high density plasma clouds traversing the radio beam at high velocities in the pulsar magnetosphere [18].

Multifrequency radio pulse profiles and single pulses from the GC magnetar revealed that the interstellar scattering is several orders of magnitude smaller than predicted by the NE2001 electron density model [52, 65, 66]. Spitler *et al.* [66] derived a scatter broadening timescale of $\tau_d = 1.3 \pm 0.2$ s at 1 GHz and a scatter broadening spectral index of $\alpha_d = -3.8 \pm 0.2$ from the scattered pulse shapes of single pulses and average pulse profiles between 1.19 and 18.95 GHz. These results were used to argue for the existence of a single uniform, thin scattering screen at a distance of $\Delta_{GC} = 5.8 \pm 0.3$ kpc from the magnetar [67]. Subse-

quent radio interferometric measurements determined that the angular and temporal broadening are both produced by a single thin scattering screen located $\sim$4.2 kpc from the magnetar [68]. However, Pearlman *et al.* [18] showed that individual single pulses from the GC magnetar at 8.4 GHz can be broadened by more than an order of magnitude compared to what is predicted by Spitler *et al.* [66], which is incompatible with a static, thin scattering screen at distances $\gtrsim 1$ kpc. A secondary local screen (e.g., $\sim$0.1 pc from the magnetar [69]) is not expected to contribute significantly to the temporal broadening [70]. We refer the interested reader to Sections 4.2 and 4.3 of Pearlman *et al.* [18] for a detailed discussion of mechanisms which might reconcile the observed pulse broadening behavior.

IV. PSR J1119–6127: A TRANSITIONAL MAGNETAR

PSR J1119–6127 is a high magnetic field ($B \approx 4 \times 10^{13}$ G), rotation-powered pulsar with a spin period of $P \approx 410$ ms [32]. The pulsar resides at the center of the supernova remnant (SNR) G292.2–0.5 [71–73], which lies in the Galactic plane at a distance of $\sim$8.4 kpc [74]. The pulsar's DM (707.4 ± 1.3 pc cm^{-3} [75]) and RM ($+853 \pm 2$ rad m^2 [76]) are both large compared to other radio pulsars (see Figure 2), and it has one of the largest period derivatives ($\dot{P} \approx 4 \times 10^{-12}$ [24]), which implies a characteristic age of $\tau_c \lesssim 2$ kyr. PSR J1119–6127 is the first rotation-powered radio pulsar to display magnetar-like activity. In fact, only one other rotation-powered X-ray pulsar, PSR J1846–0258, has previously displayed similar behavior [77], but no radio pulsations have yet been detected from that object. Short X-ray outbursts were detected from PSR J1119–6127 on 2016 July 27 and 2016 July 28 with the *Fermi* Gamma-Ray Burst Monitor (GBM) and *Swift* Burst Alert Telescope (BAT), respectively [78, 79]. A large spin-up glitch [25, 80], hardening of the X-ray spectrum [25], additional X-ray bursts [26, 35], and irregular post-outburst timing behavior [26, 81] were subsequently reported.

Shortly after the first X-ray outbursts, we used the DSN's 70 m radio telescope, DSS-43, to monitor changes in the pulsar's radio emission during this period of magnetar-like activity. Simultaneous observations were regularly performed at 2.3 and 8.4 GHz over the course of $\sim$5 months following the initial X-ray bursts. After this period, the pulsar was intermittently monitored. Several of these observations are described in detail in Majid *et al.* [32], and additional results will be presented in an upcoming paper by Pearlman *et al.* [47].

We found that radio pulsations from PSR J1119–6127 disappeared after the initial X-ray outbursts, and the emission reactivated approximately two weeks later [17, 29–32, 47, 82]. The pulse profiles at 2.3 and 8.4 GHz dramatically evolved over a time period of several months after the radio emission resumed, which is atypical of ordinary radio pulsars [17, 32, 47]. The 2.3 GHz pulse profiles developed a multicomponent emission structure, while the 8.4 GHz profile showed a single emission peak that varied in strength during this time period [17, 32, 47]. Previous radio observations per-
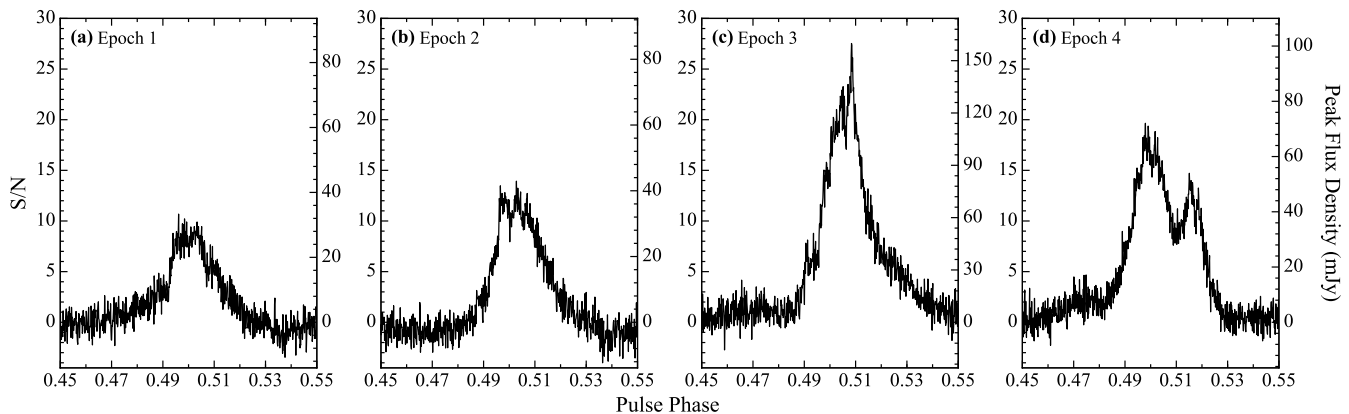
FIG. 4. Average X-band pulse profiles of the GC magnetar from observations with the 70 m DSN radio telescope, DSS-43, carried out on (a) 2015 July 30, (b) 2015 August 15, (c) 2016 April 1, and (d) 2016 August 20. This figure was adapted from Pearlman *et al.* [18].

formed before the bursts indicated that the pulse profile was predominantly single-peaked, and an extremely rare double-peaked structure was seen only once after a strong glitch in 2007 [23, 76, 83, 84]. In contrast, our post-outburst radio observations showed that the 2.3 GHz pulse profile developed multiple emission components, two of which significantly weakened several weeks after the magnetar-like activity had subsided (see Figure 6) [17, 32, 47].

Simultaneous radio observations at 2.3 and 8.4 GHz during this period revealed that the spectral index was unusually steep and comparable to the average spectral index of normal radio pulsars when the pulse profiles were multi-peaked. As the profiles stabilized and became single-peaked, the pulsar's radio spectrum flattened considerably [16, 17, 32, 47]. Significant changes in the pulsar's rotational frequency, flux density, and single pulse behavior were also observed [16, 17, 31, 32, 47]. These results demonstrate that PSR J1119–6127 is a transitional object, i.e., a high magnetic field, rotation-powered radio pulsar capable of exhibiting transient magnetar-like behavior.

The detection of pulsed radio emission from several magnetars, along with the behavior observed from PSR J1119–6127 during its 2016 outburst, has weakened the notion that there is a sharp separation between magnetars and high magnetic field, rotation-powered radio pulsars. Historically, surface dipolar magnetic fields above the quantum critical value ($B_Q = m_e^2 c^3 / e\hbar \approx 4.4 \times 10^{13}$ G) and persistent X-ray luminosities exceeding rotational energy losses ($L_x > \dot{E}$) were interpreted as some of the defining observational characteristics of magnetars, but these criteria are not always reliable predictors of magnetar-like behavior [85, 86]. In the case of PSR J1119–6127, the pulsar's quiescent X-ray luminosity in the 0.5–10 keV energy band ($L_x = 0.9 \times 10^{33}$ erg s^{-1}; Gonzalez *et al.* 87) is several orders of magnitude smaller than its spin-inferred rotational energy ($\dot{E} = 2.3 \times 10^{36}$ erg s^{-1}), i.e. $L_x/\dot{E} \approx 0.0004$, which suggests that the pulsar is often primarily powered by its rotation. However, during the 2016 outburst, the pulsar's X-ray luminosity rose to $L_x \sim 0.1\dot{E}$ [25]. Other radio magnetars, e.g. PSR J1622–

4950, XTE J1810–197, and 1E 1547.0–5408, also have X-ray conversion efficiencies below unity ($L_x/\dot{E} < 1$) [86] and display transient high-energy emission. This suggests that some magnetars and high magnetic field pulsars may be powered through a combination of magnetic and rotational energy.

V. PSR J1622–4950

PSR J1622–4950 was first detected using the Parkes radio telescope, and it is the only magnetar discovered at radio wavelengths without prior knowledge of a corresponding X-ray counterpart [8]. The pulsar has a spin period of $P \approx 4.326$ s and a DM of 820 pc cm^{-3} [8]. The timing solution, reported by Levin *et al.* [8], implies a very high surface magnetic field of $B \approx 2.8 \times 10^{14}$ G and a characteristic age of $\tau_c \approx 4$ kyr. PSR J1622–4950 has a flat radio spectrum and a highly variable flux density and pulse profile [8–10, 15, 88], which is similar to other radio magnetars.

After its initial discovery, the magnetar was regularly monitored and detected with variable flux densities at the Parkes Observatory until 2014 March [15]. Scholz *et al.* [15] resumed monitoring the magnetar in 2015 January, but they failed to detect the pulsar through 2016 September. After remaining in a dormant state for roughly 2 years, PSR J1622–4950 resumed its radio emission sometime between January and April of 2017 [89]. Shortly after the radio reactivation, we carried out simultaneous observations of PSR J1622–4950 at S-band and X-band using the 70 m radio telescope, DSS-43, on 2017 May 23 [90]. Pearlman *et al.* [90] found that the magnetar's radio spectrum had significantly steepened between 2.3 and 8.4 GHz, and its spectral behavior was consistent with the majority of ordinary pulsars.

Beginning in 2017 April, we used the 34 m DSN radio dishes near Canberra, Australia to initiate a monitoring program to observe PSR J1622–4950 over $\sim$30 epochs to date, already lasting more than a year. The observations were made using simultaneous S/X-band receivers. The data processing steps and observational setup were described in detail by Ma-

jid *et al.* [32]. The details of this monitoring campaign will be presented in Pearlman *et al.* [46]. The observing epochs were not regularly spaced during the year-long monitoring campaign due to various logistical issues, including scheduling constraints. Each observing epoch ranged in duration from roughly half an hour to four hours in length. The duration of each epoch was sufficient to obtain accurate measurements of the flux densities in both observing bands, spectral index, pulsar spin period, rate of single pulse emission, and pulse scatter broadening.

Our results indicate that the magnetar exhibited noticeable changes in its pulse profile at S-band (e.g., see Figure 7), but also particularly at X-band. PSR J1622–4950's pulse profiles sometimes showed evidence of the emergence of a new pulse component. The magnetar's flux density also showed variability in the range of a few mJy to tens of mJy. In addition, we also observed remarkable short-term changes in the magnetar's emission behavior during a few observing epochs and detected bright single pulses with varying pulse morphology (e.g., see Figure 8).

VI.   XTE J1810–197

In July 2003, XTE J1810–197 was serendipitously discovered using the *Rossi X-ray Timing Explorer* (*RXTE*) after the magnetar underwent a transient X-ray outburst [91]. The pulsar's rotational period was determined to be $P \approx 5.54$ s, and a high spin-down rate of $\dot{P} \approx 10^{-11}$ was measured, which suggests that the neutron star is young ($\tau \approx 7.6$ kyr) and possesses a large spin-inferred dipolar magnetic field ($B \approx 2.6 \times 10^{14}$ G). Approximately one year later, a coincident radio source was found at the location of the pulsar [92]. Subsequently, pulsed radio emission was detected from the magnetar, making XTE J1810–197 the first magnetar with detected radio pulsations [6]. Multifrequency radio observations between 0.7 and 42 GHz revealed that the magnetar emits bright, highly linearly polarized radio pulses, comprised of narrow sub-pulses with widths ≤ 10 ms, during each rotation [6]. These results demonstrated that there is an underlying connection between magnetars and the larger population of ordinary radio pulsars.

Radio pulsations from XTE J1810–197 suddenly ceased without warning in late 2008, despite continued X-ray activity [21, 93, 94]. After more than 10 years in quiescence, bright radio pulsations were detected again on 2018 December 8 with the 76 m Lovell Telescope at Jodrell Bank [95]. Since the magnetar's reactivation, numerous radio observatories have carried out follow-up observations of the magnetar [45, 96–100]. In particular, we observed XTE J1810–197 continuously for 5.5 hours on 2018 December 25 (MJD 58477.05623) using one of the DSN's 34 m radio telescopes near Canberra, Australia [45]. Right circular polarization data were simultaneously recorded at center frequencies of 8.4 and 32 GHz, with roughly 500 MHz of bandwidth at each frequency band, using the JPL ultra-wideband pulsar machine. Our best estimate of the barycentric spin period and DM is 5.5414471(5) s and 178 ± 9 pc cm^{-3}, respectively. The average pulse pro-

files were noticeably variable, and we detected bright, multi-component single pulses at both frequency bands. We measured mean flux densities of 4.0 ± 0.8 mJy at 8.4 GHz and 1.7 ± 0.3 mJy at 32 GHz, which yielded a spectral index of -0.7 ± 0.2 over this wide frequency range [45]. Additional multifrequency observations are needed to study the magnetar's behavior after its recent outburst. Towards this end, we are continuing to carry out high frequency radio observations of XTE J1810–197 using the DSN's 70 and 34 m radio dishes near Canberra. A regular monitoring program of this magnetar is also planned.

VII.   DISCUSSION AND CONCLUSIONS

We have presented an overview of recent results from observations of the radio magnetars, PSR J1745–2900, PSR J1622–4950, and XTE J1810–197, and the transitional magnetar candidate, PSR J1119–6127, obtained using the DSN radio telescopes near Canberra, Australia. These studies provide further evidence of the variable nature of these objects. Each of these radio magnetars exhibited remarkable pulse profile changes over timescales of weeks to months, with large accompanied flux and spectral index variations. In combination with results at X-ray wavelengths, the variability observed in radio magnetars may be explained by the conditions of the magnetosphere [4, 40, 101], though the level of variability in each object likely depends on the size and geometry of magnetospheric deformations. Toroidal oscillations in the star may be excited during an outburst, which then modify the magnetospheric structure and allow radio emission to be produced. Since this emission behavior is clearly transitory, further radio monitoring of these objects is needed to study their long-term radiative and timing behavior.

The DSN has served as an excellent facility for performing state-of-the-art pulsar observations, as we have demonstrated through the study of the four magnetars discussed in this paper. The combination of the excellent sensitivity of the DSN antennas, particularly with the presence of a large 70 m diameter dish at each of the DSN complexes, multifrequency receivers, and the recent deployment of modern pulsar machines, offers an opportunity for pulsar observations that will be a significant addition to the already existing resources in pulsar astronomy. The availability of the 70 m antenna in Canberra, with its southern location, makes it an ideal resource, complementing the Parkes telescope, for observations of Galactic plane sources, including the Galactic Center. In search mode, the DSN's pulsar machines offer high frequency and timing resolution with the ability to record multiple frequencies and incoming polarization bands simultaneously. This allows for observations with a high instantaneous sensitivity, which are quite useful for studies of single pulses. With precision tracking capabilities available at multiple frequencies, the DSN is particularly well-suited for carrying out observations at shorter wavelengths, which have proven useful for studying objects such as magnetars with flatter spectral indices and high DM pulsars.
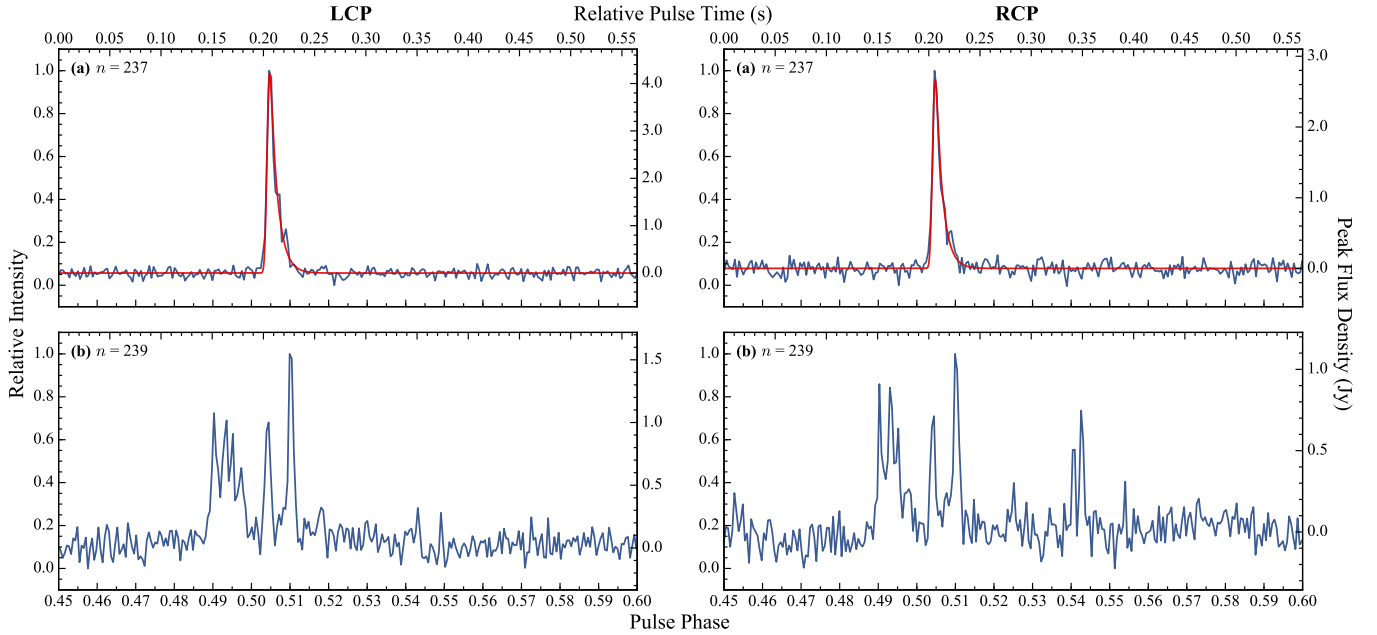
VIII.   ACKNOWLEDGMENTS

FIG. 5. Examples of bright single pulses detected from the GC magnetar at 8.4 GHz during epoch 3 (2016 April 1) with the 70 m DSN radio telescope, DSS-43. We show the single pulse profiles measured in the left circular polarization (LCP) and right circular polarization (RCP) channels during pulse cycles (a) $n = 237$ and (b) $n = 239$, where pulse numbers are referenced with respect to the start of the observation. The best-fit thin scattering screen model, described in the Appendix of Pearlman *et al.* [18], is overlaid in red on the single pulses in the top row. A pulse broadening timescale of $\tau_d^{\mathrm{LCP}} = 7.1 \pm 0.2$ ms and $\tau_d^{\mathrm{LCP}} = 6.7 \pm 0.3$ ms was measured in the corresponding polarization channels [18]. This figure was adapted from Pearlman *et al.* [18].
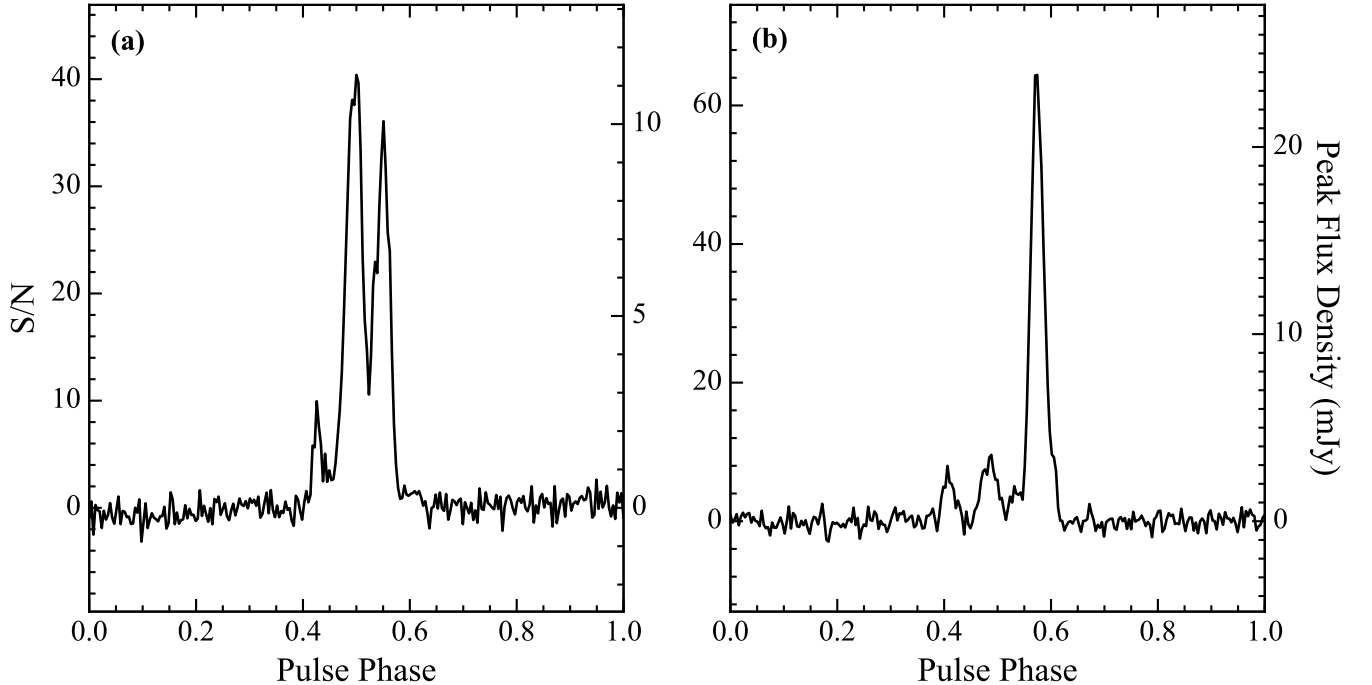

FIG. 6. Average S-band pulse profiles of PSR J1119–6127, obtained with the 70 m DSN radio telescope (DSS-43) on (a) 2016 August 19 and (b) 2016 September 1, during the pulsar's recent episode of magnetar-like activity. This figure was adapted from Majid *et al.* [32]. Additional observations during the pulsar's post-outburst recovery period will be presented in Pearlman *et al.* [47].
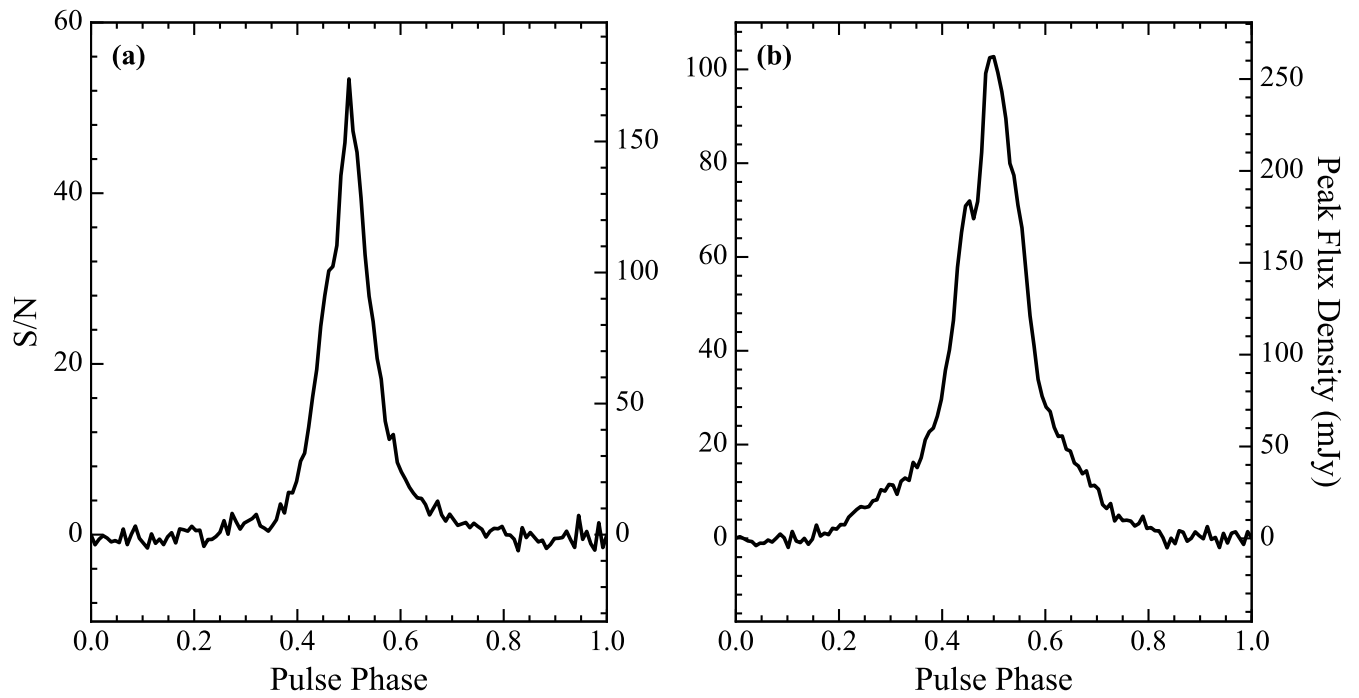
FIG. 7. Average *S*-band pulse profiles of the radio magnetar, PSR J1622–4950, obtained using the 34 m radio telescopes near Canberra, Australia on (a) 2018 April 26 and (b) 2018 May 10. Additional details on these observations will be presented in Pearlman *et al.* [46].
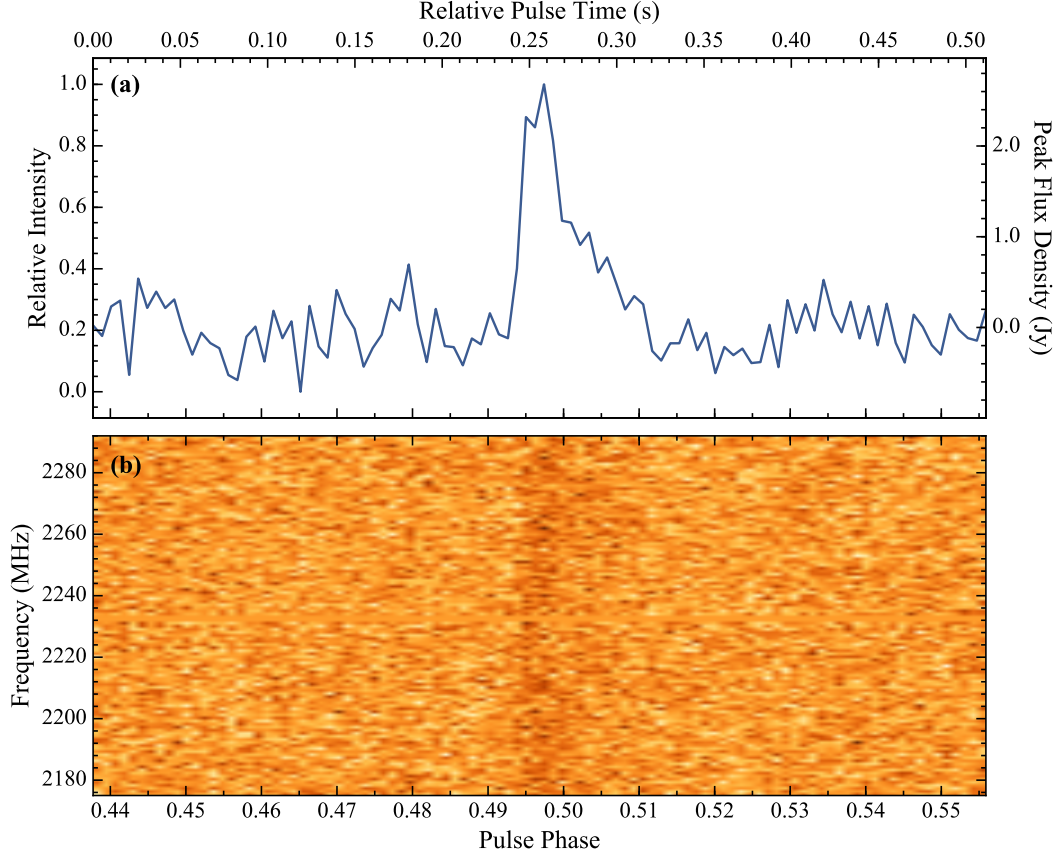
FIG. 8. Example of a bright single pulse detected at S-band from PSR J1622–4950 during the observation on 2018 May 10 (see Figure 7(b)). In panel (a), we show the integrated single pulse profile with a time resolution of $\sim$5 ms. The dynamic spectrum, dedispersed at the magnetar's nominal DM of 820 pc cm^{-3}, is shown in panel (b). This event has a S/N of $\sim$10 and was detected by convolving the dedispersed time-series with a $\sim$23 ms wide boxcar template. The shape of the single pulse is noticeably scatter-broadened.

[1] R. C. Duncan and C. Thompson, ApJL **392**, L9 (1992).

[2] C. Thompson and R. C. Duncan, MNRAS **275**, 255 (1995).

[3] C. Thompson and R. C. Duncan, ApJ **473**, 322 (1996).

[4] V. M. Kaspi and A. M. Beloborodov, ARA&A **55**, 261 (2017), arXiv:1703.00068 [astro-ph.HE].

[5] S. A. Olausen and V. M. Kaspi, ApJS **212**, 6 (2014), arXiv:1309.4167 [astro-ph.HE].

[6] F. Camilo, S. M. Ransom, J. P. Halpern, J. Reynolds, D. J. Helfand, N. Zimmerman, and J. Sarkissian, Nature **442**, 892 (2006), astro-ph/0605429.

[7] F. Camilo, S. M. Ransom, J. Peñalver, A. Karastergiou, M. H. van Kerkwijk, M. Durant, J. P. Halpern, J. Reynolds, C. Thum, D. J. Helfand, N. Zimmerman, and I. Cognard, ApJ **669**, 561 (2007), arXiv:0705.4095.

[8] L. Levin, M. Bailes, S. Bates, N. D. R. Bhat, M. Burgay, S. Burke-Spolaor, N. D'Amico, S. Johnston, M. Keith, M. Kramer, S. Milia, A. Possenti, N. Rea, B. Stappers, and W. van Straten, ApJL **721**, L33 (2010), arXiv:1007.1052 [astro-ph.HE].

[9] M. J. Keith, S. Johnston, L. Levin, and M. Bailes, MNRAS **416**, 346 (2011), arXiv:1105.3961 [astro-ph.SR].

[10] L. Levin, M. Bailes, S. D. Bates, N. D. R. Bhat, M. Burgay, S. Burke-Spolaor, N. D'Amico, S. Johnston, M. J. Keith, M. Kramer, S. Milia, A. Possenti, B. Stappers, and W. van Straten, MNRAS **422**, 2489 (2012), arXiv:1204.2045 [astro-ph.HE].

[11] P. Torne, R. P. Eatough, R. Karuppusamy, M. Kramer, G. Paubert, B. Klein, G. Desvignes, D. J. Champion, H. Wiesemeyer, C. Kramer, L. G. Spitler, C. Thum, R. Güsten, K. F. Schuster, and I. Cognard, MNRAS **451**, L50 (2015), arXiv:1504.07241 [astro-ph.HE].

[12] P. Torne, G. Desvignes, R. P. Eatough, R. Karuppusamy, G. Paubert, M. Kramer, I. Cognard, D. J. Champion, and L. G. Spitler, MNRAS **465**, 242 (2017), arXiv:1610.07616 [astro-ph.HE].

[13] F. Camilo, I. Cognard, S. M. Ransom, J. P. Halpern, J. Reynolds, N. Zimmerman, E. V. Gotthelf, D. J. Helfand, P. Demorest, G. Theureau, and D. C. Backer, ApJ **663**, 497 (2007), astro-ph/0610685.

[14] K. Lazaridis, A. Jessner, M. Kramer, B. W. Stappers, A. G. Lyne, C. A. Jordan, M. Serylak, and J. A. Zensus, MNRAS **390**, 839 (2008), arXiv:0808.0244.

[15] P. Scholz, F. Camilo, J. Sarkissian, J. E. Reynolds, L. Levin, M. Bailes, M. Burgay, S. Johnston, M. Kramer, and A. Possenti, ApJ **841**, 126 (2017), arXiv:1705.04899 [astro-ph.HE].

[16] A. B. Pearlman, W. A. Majid, S. Horiuchi, J. Kocz, J. Lippuner, and T. A. Prince, The Astronomer's Telegram **9870** (2016).

[17] A. B. Pearlman, W. A. Majid, S. Horiuchi, J. Kocz, J. Lippuner, and T. A. Prince, in *AAS/High Energy Astrophysics Division #16*, AAS/High Energy Astrophysics Division, Vol. 16 (2017) p. 109.17.

[18] A. B. Pearlman, W. A. Majid, T. A. Prince, J. Kocz, and S. Horiuchi, ApJ **866**, 160 (2018), arXiv:1809.02140 [astro-ph.HE].

[19] F. Camilo, J. Reynolds, S. Johnston, J. P. Halpern, S. M. Ransom, and W. van Straten, ApJL **659**, L37 (2007), astro-ph/0702616.

[20] F. Camilo, J. Reynolds, S. Johnston, J. P. Halpern, and S. M. Ransom, ApJ **679**, 681-686 (2008), arXiv:0802.0494.

[21] F. Camilo, S. M. Ransom, J. P. Halpern, J. A. J. Alford, I. Cognard, J. E. Reynolds, S. Johnston, J. Sarkissian, and W. van Straten, ApJ **820**, 110 (2016), arXiv:1603.02170 [astro-ph.SR].

[22] J. M. Cordes, N. D. R. Bhat, T. H. Hankins, M. A. McLaughlin, and J. Kern, ApJ **612**, 375 (2004), astro-ph/0304495.

[23] P. Weltevrede, S. Johnston, and C. M. Espinoza, MNRAS **411**, 1917 (2011), arXiv:1010.0857 [astro-ph.SR].

[24] D. Antonopoulou, P. Weltevrede, C. M. Espinoza, A. L. Watts, S. Johnston, R. M. Shannon, and M. Kerr, MNRAS **447**, 3924 (2015), arXiv:1412.5853 [astro-ph.HE].

[25] R. F. Archibald, V. M. Kaspi, S. P. Tendulkar, and P. Scholz, ApJL **829**, L21 (2016), arXiv:1608.01007 [astro-ph.HE].

[26] R. F. Archibald, V. M. Kaspi, S. P. Tendulkar, and P. Scholz, ApJ **869**, 180 (2018), arXiv:1806.01414 [astro-ph.HE].

[27] M. Burgay, G. L. Israel, A. Possenti, N. Rea, P. Esposito, S. Mereghetti, A. Tiengo, and D. Gotz, The Astronomer's Telegram **1913** (2009).

[28] F. Camilo, J. P. Halpern, and S. M. Ransom, The Astronomer's Telegram **1907** (2009).

[29] M. Burgay, A. Possenti, M. Kerr, P. Esposito, N. Rea, F. C. Zelati, G. L. Israel, and S. Johnston, The Astronomer's Telegram **9286** (2016).

[30] M. Burgay, A. Possenti, M. Kerr, P. Esposito, N. Rea, F. C. Zelati, G. L. Israel, and S. Johnston, The Astronomer's Telegram **9366** (2016).

[31] W. Majid, T. Dobreva, J. Kocz, J. Lazio, J. Lippuner, A. B. Pearlman, and T. Prince, The Astronomer's Telegram **9321** (2016).

[32] W. A. Majid, A. B. Pearlman, T. Dobreva, S. Horiuchi, J. Kocz, J. Lippuner, and T. A. Prince, ApJL **834**, L2 (2017), arXiv:1612.02868 [astro-ph.HE].

[33] N. Degenaar, M. T. Reynolds, J. M. Miller, J. A. Kennea, and R. Wijnands, The Astronomer's Telegram **5006** (2013).

[34] J. A. Kennea, D. N. Burrows, C. Kouveliotou, D. M. Palmer, E. Göğüş, Y. Kaneko, P. A. Evans, N. Degenaar, M. T. Reynolds, J. M. Miller, R. Wijnands, K. Mori, and N. Gehrels, ApJL **770**, L24 (2013), arXiv:1305.2128 [astro-ph.HE].

[35] E. Göğüş, L. Lin, Y. Kaneko, C. Kouveliotou, A. L. Watts, M. Chakraborty, M. A. Alpar, D. Huppenkothen, O. J. Roberts, G. Younes, and A. J. van der Horst, ApJL **829**, L25 (2016), arXiv:1608.07133 [astro-ph.HE].

[36] P. M. Woods and C. Thompson, "Soft gamma repeaters and anomalous X-ray pulsars: magnetar candidates," in *Compact stellar X-ray sources*, edited by W. H. G. Lewin and M. van der Klis (2006) pp. 547–586.

[37] V. M. Kaspi, Proceedings of the National Academy of Science **107**, 7147 (2010), arXiv:1005.0876 [astro-ph.HE].

[38] N. Rea and P. Esposito, Astrophysics and Space Science Proceedings **21**, 247 (2011), arXiv:1101.4472.

[39] S. Mereghetti, J. A. Pons, and A. Melatos, Space Sci. Rev. **191**, 315 (2015), arXiv:1503.06313 [astro-ph.HE].

[40] R. Turolla, S. Zane, and A. L. Watts, Reports on Progress in Physics **78**, 116901 (2015), arXiv:1507.02924 [astro-ph.HE].

[41] V. M. Kaspi and M. Kramer, ArXiv e-prints (2016), arXiv:1602.07738 [astro-ph.HE].

[42] R. N. Manchester, G. B. Hobbs, A. Teoh, and M. Hobbs, AJ **129**, 1993 (2005), astro-ph/0412641.

[43] B. Zhang, A. K. Harding, and A. G. Muslimov, ApJL **531**, L135 (2000), astro-ph/0001341.

[44] E. Petroff, E. D. Barr, A. Jameson, E. F. Keane, M. Bailes, M. Kramer, V. Morello, D. Tabbara, and W. van Straten, PASA **33**, e045 (2016), arXiv:1601.03547 [astro-ph.HE].

[45] W. A. Majid, A. B. Pearlman, T. A. Prince, S. Horiuchi, C. J. Naudet, J. Kocz, and T. Enoto, The Astronomer's Telegram **12353**, 1 (2019).

[46] A. B. Pearlman, A. Cook, A. Amsellem, Z. Arzoumanian, T. Enoto, K. C. Gendreau, S. Horiuchi, J. Kocz, W. A. Majid, C. J. Naudet, and T. A. Prince, In Preparation (2019).

[47] A. B. Pearlman, W. A. Majid, and T. A. Prince, et al., In Preparation (2019).

[48] W. A. Majid, C. J. Naudet, S. T. Lowe, and T. B. H. Kuiper, ApJ **741**, 53 (2011), arXiv:1108.2307.

[49] W. Majid, in *Neutron Stars and Pulsars: Challenges and Opportunities after 80 years*, IAU Symposium, Vol. 291, edited by J. van Leeuwen (2013) pp. 322–322.

[50] R. P. Eatough, H. Falcke, R. Karuppusamy, K. J. Lee, D. J. Champion, E. F. Keane, G. Desvignes, D. H. F. M. Schnitzeler, L. G. Spitler, M. Kramer, B. Klein, C. Bassa, G. C. Bower, A. Brunthaler, I. Cognard, A. T. Deller, P. B. Demorest, P. C. C. Freire, A. Kraus, A. G. Lyne, A. Noutsos, B. Stappers, and N. Wex, Nature **501**, 391 (2013), arXiv:1308.3147 [astro-ph.GA].

[51] G. C. Bower, A. Deller, P. Demorest, A. Brunthaler, H. Falcke, M. Moscibrodzka, R. M. O'Leary, R. P. Eatough, M. Kramer, K. J. Lee, L. Spitler, G. Desvignes, A. P. Rushton, S. Doeleman, and M. J. Reid, ApJ **798**, 120 (2015), arXiv:1411.0399 [astro-ph.HE].

[52] T. T. Pennucci, A. Possenti, P. Esposito, N. Rea, D. Haggard, F. K. Baganoff, M. Burgay, F. Coti Zelati, G. L. Israel, and A. Minter, ApJ **808**, 81 (2015), arXiv:1505.00836 [astro-ph.HE].

[53] O. Maron, J. Kijak, M. Kramer, and R. Wielebinski, A&AS **147**, 195 (2000), astro-ph/0010233.

[54] R. S. Lynch, R. F. Archibald, V. M. Kaspi, and P. Scholz, ApJ **806**, 266 (2015), arXiv:1412.0610 [astro-ph.HE].

[55] M. Serylak, B. W. Stappers, P. Weltevrede, M. Kramer, A. Jessner, A. G. Lyne, C. A. Jordan, K. Lazaridis, and J. A. Zensus, MNRAS **394**, 295 (2009), arXiv:0811.3829.

[56] Z. Yan, Z.-Q. Shen, X.-J. Wu, R. N. Manchester, P. Weltevrede, Y.-J. Wu, R.-B. Zhao, J.-P. Yuan, K-J. Lee, Q.-Y. Fan, X.-Y. Hong, D.-R. Jiang, B. Li, S.-G. Liang, Q.-B. Ling, Q.-H. Liu, Z.-H. Qian, X.-Z. Zhang, W.-Y. Zhong, and S.-H. Ye, ApJ **814**, 5 (2015), arXiv:1510.00183 [astro-ph.HE].

[57] J. D. Gelfand, S. Ransom, C. Kouveliotou, J. Granot, A. J. van der Horst, G. Zhang, E. Göğüş, M. S. E. Roberts, and H. A. Ali, ApJ **850**, 53 (2017), arXiv:1711.10187 [astro-ph.HE].

[58] W. M. Yan, N. Wang, R. N. Manchester, Z. G. Wen, and J. P. Yuan, MNRAS **476**, 3677 (2018), arXiv:1802.07884 [astro-ph.HE].

[59] T. H. Hankins, J. A. Eilek, and G. Jones, ApJ **833**, 47 (2016), arXiv:1608.08881 [astro-ph.HE].

[60] L. G. Spitler, P. Scholz, J. W. T. Hessels, S. Bogdanov, A. Brazier, F. Camilo, S. Chatterjee, J. M. Cordes, F. Crawford, J. Deneva, R. D. Ferdman, P. C. C. Freire, V. M. Kaspi, P. Lazarus, R. Lynch, E. C. Madsen, M. A. McLaughlin, C. Patel, S. M. Ransom, A. Seymour, I. H. Stairs, B. W. Stappers, J. van Leeuwen, and W. W. Zhu, Nature **531**, 202 (2016), arXiv:1603.00581 [astro-ph.HE].

[61] V. Gajjar, A. P. V. Siemion, D. C. Price, C. J. Law, D. Michilli, J. W. T. Hessels, S. Chatterjee, A. M. Archibald, G. C. Bower, C. Brinkman, S. Burke-Spolaor, J. M. Cordes, S. Croft, J. E. Enriquez, G. Foster, N. Gizani, G. Hellbourg, H. Isaacson, V. M. Kaspi, T. J. W. Lazio, M. Lebofsky, R. S. Lynch, D. MacMahon, M. A. McLaughlin, S. M. Ransom, P. Scholz, A. Seymour, L. G. Spitler, S. P. Tendulkar, D. Werthimer, and Y. G. Zhang, ApJ **863**, 2 (2018), arXiv:1804.04101 [astro-

[62] D. Michilli, A. Seymour, J. W. T. Hessels, L. G. Spitler, V. Gajjar, A. M. Archibald, G. C. Bower, S. Chatterjee, J. M. Cordes, K. Gourdji, G. H. Heald, V. M. Kaspi, C. J. Law, C. Sobey, E. A. K. Adams, C. G. Bassa, S. Bogdanov, C. Brinkman, P. Demorest, F. Fernandez, G. Hellbourg, T. J. W. Lazio, R. S. Lynch, N. Maddox, B. Marcote, M. A. McLaughlin, Z. Paragi, S. M. Ransom, P. Scholz, A. P. V. Siemion, S. P. Tendulkar, P. van Rooy, R. S. Wharton, and D. Whitlow, Nature **553**, 182 (2018), arXiv:1801.03965 [astro-ph.HE].

[63] U.-L. Pen and L. Connor, ApJ **807**, 179 (2015), arXiv:1501.01341 [astro-ph.HE].

[64] B. D. Metzger, E. Berger, and B. Margalit, ApJ **841**, 14 (2017), arXiv:1701.02370 [astro-ph.HE].

[65] J. M. Cordes and T. J. W. Lazio, ArXiv Astrophysics e-prints (2002), astro-ph/0207156.

[66] L. G. Spitler, K. J. Lee, R. P. Eatough, M. Kramer, R. Karuppusamy, C. G. Bassa, I. Cognard, G. Desvignes, A. G. Lyne, B. W. Stappers, G. C. Bower, J. M. Cordes, D. J. Champion, and H. Falcke, ApJL **780**, L3 (2014), arXiv:1309.4673 [astro-ph.HE].

[67] G. C. Bower, A. Deller, P. Demorest, A. Brunthaler, R. Eatough, H. Falcke, M. Kramer, K. J. Lee, and L. Spitler, ApJL **780**, L2 (2014), arXiv:1309.4672.

[68] O. Wucknitz, in *Proceedings of the 12th European VLBI Network Symposium and Users Meeting*, PoS, Vol. 66, edited by A. Tarchi, M. Giroletti, and L. Feretti (Trieste: SISSA, 2014) pp. 1–6.

[69] G. Desvignes, R. P. Eatough, U. L. Pen, K. J. Lee, S. A. Mao, R. Karuppusamy, D. H. F. M. Schnitzeler, H. Falcke, M. Kramer, O. Wucknitz, L. G. Spitler, P. Torne, K. Liu, G. C. Bower, I. Cognard, A. G. Lyne, and B. W. Stappers, ApJL **852**, L12 (2018), arXiv:1711.10323 [astro-ph.HE].

[70] J. Dexter, A. Deller, G. C. Bower, P. Demorest, M. Kramer, B. W. Stappers, A. G. Lyne, M. Kerr, L. G. Spitler, D. Psaltis, M. Johnson, and R. Narayan, MNRAS **471**, 3563 (2017), arXiv:1707.03842.

[71] F. Crawford, B. M. Gaensler, V. M. Kaspi, R. N. Manchester, F. Camilo, A. G. Lyne, and M. J. Pivovaroff, ApJ **554**, 152 (2001), astro-ph/0012287.

[72] M. J. Pivovaroff, V. M. Kaspi, F. Camilo, B. M. Gaensler, and F. Crawford, ApJ **554**, 161 (2001), astro-ph/0102084.

[73] H. S. Kumar, S. Safi-Harb, and M. E. Gonzalez, ApJ **754**, 96 (2012), arXiv:1205.5766 [astro-ph.HE].

[74] J. L. Caswell, N. M. McClure-Griffiths, and M. C. M. Cheung, MNRAS **352**, 1405 (2004).

[75] C. He, C.-Y. Ng, and V. M. Kaspi, ApJ **768**, 64 (2013), arXiv:1303.5170 [astro-ph.HE].

[76] S. Johnston and J. M. Weisberg, MNRAS **368**, 1856 (2006), astro-ph/0603037.

[77] F. P. Gavriil, M. E. Gonzalez, E. V. Gotthelf, V. M. Kaspi, M. A. Livingstone, and P. M. Woods, Science **319**, 1802 (2008), arXiv:0802.1704 [astro-ph].

[78] J. A. Kennea, A. Y. Lien, F. E. Marshall, D. M. Palmer, T. G. R. Roegiers, and B. Sbarufatti, The Astronomer's Telegram **9274** (2016).

[79] G. Younes, C. Kouveliotou, and O. Roberts, GRB Coordinates Network, Circular Service, No. 19736, #1 (2016) **19736** (2016).

[80] R. F. Archibald, S. P. Tendulkar, P. A. Scholz, and V. M. Kaspi, The Astronomer's Telegram **9284** (2016).

[81] L. C.-C. Lin, H.-H. Wang, K.-L. Li, J. Takata, C.-P. Hu, C.-Y. Ng, C. Y. Hui, A. K. H. Kong, P.-H. T. Tam, and P. K. H.

Yeung, ApJ **866**, 6 (2018), arXiv:1806.02017 [astro-ph.HE].

[82] S. Dai, S. Johnston, P. Weltevrede, M. Kerr, M. Burgay, P. Esposito, G. Israel, A. Possenti, N. Rea, and J. Sarkissian, MNRAS **480**, 3584 (2018), arXiv:1806.05064 [astro-ph.HE].

[83] F. Camilo, V. M. Kaspi, A. G. Lyne, R. N. Manchester, J. F. Bell, N. D'Amico, N. P. F. McKay, and F. Crawford, ApJ **541**, 367 (2000), astro-ph/0004330.

[84] F. Crawford and N. C. Keim, ApJ **590**, 1020 (2003), astro-ph/0303082.

[85] S. Mereghetti, A&A Rev. **15**, 225 (2008), arXiv:0804.0250.

[86] N. Rea, J. A. Pons, D. F. Torres, and R. Turolla, ApJL **748**, L12 (2012), arXiv:1202.3069 [astro-ph.GA].

[87] M. E. Gonzalez, V. M. Kaspi, F. Camilo, B. M. Gaensler, and M. J. Pivovaroff, ApJ **630**, 489 (2005), astro-ph/0505332.

[88] G. E. Anderson, B. M. Gaensler, P. O. Slane, N. Rea, D. L. Kaplan, B. Posselt, L. Levin, S. Johnston, S. S. Murray, C. L. Brogan, M. Bailes, S. Bates, R. A. Benjamin, N. D. R. Bhat, M. Burgay, S. Burke-Spolaor, D. Chakrabarty, N. D'Amico, J. J. Drake, P. Esposito, J. E. Grindlay, J. Hong, G. L. Israel, M. J. Keith, M. Kramer, T. J. W. Lazio, J. C. Lee, J. C. Mauerhan, S. Milia, A. Possenti, B. Stappers, and D. T. H. Steeghs, ApJ **751**, 53 (2012), arXiv:1203.2719 [astro-ph.HE].

[89] F. Camilo, P. Scholz, M. Serylak, S. Buchner, M. Merryfield, V. M. Kaspi, R. F. Archibald, M. Bailes, A. Jameson, W. van Straten, and et al., ApJ **856**, 180 (2018), arXiv:1804.01933 [astro-ph.HE].

[90] A. B. Pearlman, W. A. Majid, T. A. Prince, S. Horiuchi, J. Kocz, T. J. W. Lazio, and C. J. Naudet, The Astronomer's Telegram **10581** (2017).

[91] A. I. Ibrahim, C. B. Markwardt, J. H. Swank, S. Ransom, M. Roberts, V. Kaspi, P. M. Woods, S. Safi-Harb, S. Balman, W. C. Parke, C. Kouveliotou, K. Hurley, and T. Cline, ApJL **609**, L21 (2004), astro-ph/0310665.

[92] J. P. Halpern, E. V. Gotthelf, R. H. Becker, D. J. Helfand, and R. L. White, ApJL **632**, L29 (2005), astro-ph/0508534.

[93] F. Pintore, F. Bernardini, S. Mereghetti, P. Esposito, R. Turolla, N. Rea, F. Coti Zelati, G. L. Israel, A. Tiengo, and S. Zane, MNRAS **458**, 2088 (2016), arXiv:1602.03359 [astro-ph.HE].

[94] F. Pintore, S. Mereghetti, P. Esposito, R. Turolla, A. Tiengo, N. Rea, F. Bernardini, and G. L. Israel, MNRAS **483**, 3832 (2019), arXiv:1812.03153 [astro-ph.HE].

[95] A. Lyne, L. Levin, B. Stappers, M. Mickaliger, G. Desvignes, and M. Kramer, The Astronomer's Telegram **12284** (2018).

[96] G. Desvignes, R. Eatough, M. Kramer, R. Karuppusamy, A. Kraus, A. Lyne, L. Levin, B. Stappers, and M. Mickaliger, The Astronomer's Telegram **12285** (2018).

[97] M. E. Lower, M. Bailes, A. Jameson, W. Farah, C. Flynn, V. Gupta, T. Bateman, E. D. Barr, S. Bhandari, M. Caleb, D. Campbell-Wilson, C. Day, A. Deller, A. J. Green, R. W. Hunstead, F. Jankowski, E. F. Keane, S. Oslowski, A. Parthasarathy, K. Plant, D. C. Price, V. Ravi, R. M. Shannon, A. Sutherland, D. Temby, G. Torr, G. Urquhart, V. V. Krishnan, and T. Venville, The Astronomer's Telegram **12288** (2018).

[98] B. C. Joshi, Y. Maan, M. P. Surnis, M. Bagchi, and P. K. Manoharan, The Astronomer's Telegram **12312** (2018).

[99] S. Del Palacio, F. Garcia, L. Combi, F. Lopez Armengol, G. Gancio, A. L. Muller, and P. Kornecki, The Astronomer's Telegram **12323** (2018).

[100] S. A. Trushkin, N. N. Bursov, P. G. Tsybulev, N. A. Nizhelskij, and A. Erkenov, The Astronomer's Telegram **12372** (2019).

[101] R. F. Archibald, M. Burgay, M. Lyutikov, V. M. Kaspi, P. Esposito, G. Israel, M. Kerr, A. Possenti, N. Rea, J. Sarkissian, P. Scholz, and S. P. Tendulkar, ApJL **849**, L20 (2017), arXiv:1710.03718 [astro-ph.HE].